0026-895X/11/7902-262–269$20.00
MOLECULAR PHARMACOLOGY
Vol. 79, No. 2
66068/3662885
Mol Pharmacol 79:262–269, 2011
Printed in U.S.A.
Copyright © 2011 The American Society for Pharmacology and Experimental Therapeutics

A Structural Insight into the Reorientation of Transmembrane Domains 3 and 5 during Family A G Protein-Coupled Receptor Activation[S]

Kamonchanok Sansuk, Xavier Deupi,[1] Ivan R. Torrecillas, Aldo Jongejan, Saskia Nijmeijer, Remko A. Bakker,[2] Leonardo Pardo, and Rob Leurs

Leiden/Amsterdam Center for Drug Research, Department of Medicinal Chemistry, Vrije Universiteit Amsterdam, Amsterdam, the Netherlands (K.S., A.J., S.N., R.A.B., R.L.); and Laboratori de Medicina Computacional, Unitat de Bioestadística, Facultat de Medicina, Universitat Autònoma de Barcelona, Bellaterra, Spain (X.D., I.R.T., L.P.)

Received May 5, 2010; accepted November 16, 2010

ABSTRACT

Rearrangement of transmembrane domains (TMs) 3 and 5 after agonist binding is necessary for stabilization of the active state of class A G protein-coupled receptors (GPCRs). Using site-directed mutagenesis and functional assays, we provide the first evidence that the TAS(I/V) sequence motif at positions 3.37 to 3.40, highly conserved in aminergic receptors, plays a key role in the activation of the histamine H_1 receptor. By combining these data with structural information from X-ray crystallography and computational modeling, we suggest that $Thr^{3.37}$ interacts with TM5, stabilizing the inactive state of the receptor, whereas the hydrophobic side chain at position 3.40, highly conserved in the whole class A GPCR family, facilitates the reorientation of TM5. We propose that the structural change of TM5 during the process of GPCR activation involves a local $Pro^{5.50}$-induced unwinding of the helix, acting as a hinge, and the highly conserved hydrophobic $Ile^{3.40}$ side chain, acting as a pivot.

Introduction

G protein-coupled receptors (GPCRs) transduce sensory signals of external origin such as photons, odors, or pheromones and endogenous signals, including biogenic amines, (neuro)peptides, proteases, glycoprotein hormones, and ions, to the cytoplasmic side of the cell membrane (Kristiansen, 2004). The mechanism by which binding of these highly diverse chemical signals triggers a set of conformational rearrangements of the transmembrane (TM) segments near the G-protein binding domains remains largely unknown. Nevertheless, comparison of the structure of inactive rhodopsin (Li et al., 2004) with the recent crystal structure of the ligand-free opsin (Park et al., 2008), which contains several distinctive features of the presumed active state, leads to conclude that during the process of GPCR activation, among other changes, TM3 rotates clockwise (viewed from the intracellular side), the intracellular part of TM6 tilts outwards by 6 to 7 Å, TM5 approaches TM6, and $Arg^{3.50}$ (see *Materials and Methods* for the general numbering scheme) within the (D/E)R(Y/W) motif in TM3 adopts an extended conformation pointing toward the protein core (Park et al., 2008). Notably, as revealed in the original publication of the opsin crystal structure, these conformational changes disrupt the ionic interaction between $Arg^{3.50}$ with negatively charged side chains at positions 3.49 and 6.30 [Smit et al. (2007) and Rosenbaum et al. (2009) discuss conserved amino acids involved in GPCR activation] and facilitate the interactions between the highly conserved $Tyr^{5.58}$ and $Lys^{5.66}$ in TM5 and $Arg^{3.50}$ in TM3 and $Glu^{6.30}$ in TM6, respectively. These structural changes strongly suggest that both TMs 3 and 5 play a central role in stabilizing the active state of GPCRs and, therefore, in the process of GPCR activation.

In this study, we have combined the latest structural insights in GPCR structure, computational modeling, and site-

This work was supported by the Ministerio de Educación y Ciencia [Grant SAF2010-22198-C02-02]; the Instituto de Salud Carlos III [Grant RD07/0067/0008]; and the Ministerio de Educación y Ciencia through the Ramon y Cajal program (to X.D.).

K.S. and X.D. contributed equally to this work.

[1] Current affiliation: Condensed Matter Theory Group and Laboratory of Biomolecular Research, Paul Scherrer Institut, Villigen PSI, Switzerland.

[2] Current affiliation: Boehringer Ingelheim Pharma GmbH and Co. KG, Biberach, Germany.

Article, publication date, and citation information can be found at http://molpharm.aspetjournals.org.
doi:10.1124/mol.110.066068.

[S] The online version of this article (available at http://molpharm.aspetjournals.org) contains supplemental material.

ABBREVIATIONS: GPCR, G protein-coupled receptor; H_1R, H_1 receptor; WT, wild type; TM, transmembrane; *t, trans*; *g+, gauche+*; *g−, gauche−*; NF-κB, nuclear factor κB.

directed mutagenesis to study the role of the TAS(I/V) motif at positions 3.37 to 3.40 in TM3, highly conserved in aminergic receptors, in the process of receptor activation. Our results suggest that $Thr^{3.37}$ interacts with TM5 in the inactive state of the receptor. In addition, we provide the first evidence that the hydrophobic side chain at position 3.40, highly conserved in the whole class A of GPCRs, plays a key role in activation. Mutation of $Ile^{3.40}$ to either alanine or glycine (i.e., removing the bulky side chain at this position) abolishes the constitutive activity of the histamine H_1 receptor (H_1R), the effect of constitutive-activity increasing mutations, and the histamine-induced receptor activation.

Materials and Methods

Materials. Gifts of mianserin hydrochloride (Organon NV, Oss, The Netherlands), $pcDEF_3$ (Dr. J. Langer; Goldman et al., 1996), and the cDNA encoding the human histamine H_1R (Dr. H. Fukui; Fukui et al., 1994) are greatly acknowledged. pNF-κB-Luc was obtained from Stratagene (La Jolla, CA), ATP disodium salt, bovine serum albumin, chloroquine diphosphate, DEAE-dextran (chloride form), histamine dihydrochloride, mepyramine (pyrilamine maleate), and polyethylenimine were purchased from Sigma-Aldrich (St. Louis, MO). D-Luciferin was obtained from Duchefa Biochemie BV (Haarlem, The Netherlands), glycerol from Riedel-de-Haen (Seelze, Germany), and Triton X-100 from Fluka (Buchs, Switzerland). Cell culture media, penicillin, and streptomycin were obtained from Invitrogen (Carlsbad, CA). Fetal bovine serum was obtained from Intergro B.V. (Zaandam, the Netherlands). Cell culture plastics were obtained from Corning Life Sciences (Lowell, MA). [^{3}H]Mepyramine (30 Ci/mmol) was purchased-from MP Biomedicals (Solon, OH).

Cell Culture and Transfection. COS-7 African green monkey kidney cells were maintained at 37°C in a humidified 5% CO_2/95% air atmosphere in Dulbecco's modified Eagle's medium containing 50 IU/ml penicillin, 50 μg/ml streptomycin, and 5% (v/v) fetal bovine serum. COS-7 cells were transiently transfected using the DEAE-dextran method as described previously (Bakker et al., 2001).

Site-Directed Mutagenesis. Single-point mutant human histamine H_1Rs $T^{3.37}A$, $T^{3.37}E$, $I^{3.40}A$, and $I^{3.40}G$ and double mutant human histamine H_1Rs $S^{3.36}T/I^{3.40}A$, $S^{3.36}T/I^{3.40}G$, $I^{6.40}K/I^{3.40}A$, and $I^{6.40}S/I^{3.40}A$ were created using a polymerase chain reaction-based mutagenesis approach. All constructs were subcloned into the expression vector $pcDEF_3$ and were verified by DNA sequencing.

Reporter-Gene Assay. Reporter-gene assays were performed essentially as described previously (Bakker et al., 2001). In brief, cells transiently cotransfected with pNF-κB-Luc (125 μg/1.10^7 cells) and $pcDEF_3$ encoding wild-type (WT) or mutant H_1Rs (25 μg/1.10^7 cells) were seeded in 96-well white plates (Corning Life Sciences) in serum-free culture medium and incubated with drugs. After 48 h, cells were assayed for luminescence by aspiration of the medium and the addition of 25 μl/well luciferase assay reagent [0.83 mM ATP, 0.83 mM D-luciferin, 18.7 mM $MgCl_2$, 0.78 μM $Na_2H_2P_2O_7$, 38.9 mM Tris, pH 7.8. 0.39% (v/v) glycerol, 0.03% (v/v) Triton X-100, and 2.6 μM dithiothreitol]. After 30 min, luminescence was measured for 3 s/well in a Victor^2 plate reader (PerkinElmer Life and Analytical Sciences, Waltham, MA). Structural rearrangements during GPCR activation probably occur on a millisecond time scale and, therefore, this assay cannot assess the influence of the mutations on these fast processes. However, we show that specific mutations disrupt receptor activation, probably by stabilizing nonfunctional conformations. We are able to detect these types of disruptions by measuring the changes in receptor signaling in the reporter-gene assay. This assay has been shown to be comparable with the classic G_q-linked generation of inositol phosphates (Bakker et al., 2001).

Histamine H_1R Binding Studies. Histamine H_1R binding studies were performed essentially as described previously (Bakker et al., 2001). In brief, transfected COS-7 cells used for radioligand binding studies were harvested after 48 h and homogenized in 50 mM ice-cold Na_2/potassium phosphate buffer, pH 7.4 (binding buffer). The COS-7 cell homogenates were incubated for 30 min at 30°C in binding buffer in 200 μl with 3 nM [^{3}H]mepyramine. Nonspecific binding was determined in the presence of 1 μM mianserin. The incubations were stopped by rapid dilution with 3 ml of ice-cold binding buffer. The bound radioactivity was separated by filtration through Whatman GF/C filters that had been treated with 0.3% polyethyleneimine. Filters were washed twice with 3 ml of binding buffer, and the radioactivity retained on the filters was measured by liquid scintillation counting.

Analytical Methods. Protein concentrations were determined according to Bradford's method (Bradford, 1976), using bovine serum albumin as a standard. Binding and functional data were evaluated by a nonlinear, least-squares curve-fitting procedure using GraphPad Prism 4 (GraphPad Software, Inc., San Diego, CA).

Computational Model of the Histamine H_1R. A model of the TM domains 1 to 7 of the histamine H_1R was built by homology modeling using the crystal structure of the β_2-adrenergic receptor (Protein Data Bank code 2RH1) (Rosenbaum et al., 2007) as template. Building this homology model was straightforward except for the highly conserved $NPxxY{x}_{n\,=\,5,6}F$ motif at the junction between TM7 and the intracellular helix 8. Notably, this junction is one residue shorter in the β_2-adrenergic receptor ($n = 5$) than in rhodopsin ($n = 6$). As a result, $Tyr^{7.53}$ is pointing toward TM2 in rhodopsin (Li et al., 2004) and toward TM6 in the β_2-adrenergic receptor (Rosenbaum et al., 2007). The fact that the histamine H_1R contains six amino acids ($n = 6$) between both aromatic side chains led us to model the junction between TM7 and helix 8 as in rhodopsin (Protein Data Bank code 1GZM). Modeler 9v1 (Martí-Renom et al., 2000) was used to add intracellular loops 1 to 2 and extracellular loops 1 to 3 using the structure of the β_2-adrenergic receptor as template. Internal water molecules 506, 519, 528, 529, 532, 534, 537, 543, 546, and 548 that mediate a number of key interhelical interactions (Rosenbaum et al., 2007) and are probably conserved in family A GPCRs (Pardo et al., 2007) were explicitly included in the model.

Distortion of TM5. The program HELANAL (Bansal et al., 2000) was used to calculate the residue unit twist angle of TM5, a structural parameter that describes local helical uniformity. This parameter is interpreted as follows: an ideal α-helix, with approximately 3.6 residues per turn, has a twist angle of approximately 100° (360°/3.6); a closed helical segment, with <3.6 residues per turn, possesses a twist >100°; whereas an open helical segment, with >3.6 residues per turn, possesses a twist <100°.

Nomenclature of Side Chain Conformation. The side chain conformations have been categorized into *gauche*− (*g*−: $0° < \chi_1 < 120°$), *trans* (*t*: $120° < \chi_1 < 240°$), or *gauche*+ (*g*+: $240° < \chi_1 < 360°$) depending on the value of the χ_1 torsional angle.

Numbering Scheme of GPCRs. Residues are identified by the general numbering scheme of Ballesteros and Weinstein (1995) that allows easy comparison among residues in the 7TM segments of different receptors.

Sequence Analysis. Family-specific analyses of GPCR sequence conservation were performed using the GMoS program (http://lmc.uab.cat/gmos).

Results

A Proline-Induced Unwinding in the Structure of TM5 of Class A GPCRs. GPCRs possess a highly conserved $Pro^{5.50}$ in TM5, present in 77% of the rhodopsin-like sequences, absent only in melanocortin, glycoprotein hormone, lysosphingolipid, prostanoid, and cannabinoid receptors. Usually, in proline-containing α-helices, the steric clash between the pyrrolidine ring of proline and the backbone carbonyl oxygen in the preceding turn induces a bend angle of approximately 20° in the helical structure (Deupi et al., 2004). How-

ever, a detailed analysis of the structures of bovine (Li et al., 2004) and squid (Murakami and Kouyama, 2008) rhodopsin, adenosine A_{2A} receptor (Jaakola et al., 2008), and the β_1- (Warne et al., 2008) and β_2- (Rosenbaum et al., 2007) adrenergic receptors has allowed us to detect and quantify a peculiar distortion of TM5 in which a local opening of the helix (>3.6 residues/turn, twist <100°, see *Materials and Methods*) at the 5.45 to 5.48 turn (Fig. 1B) partially removes the steric clash between the pyrrolidine ring of $Pro^{5.50}$ and the backbone carbonyl oxygen at position 5.46 (i-4 in Fig. 1, C–H). This local opening of TM5 (proline-unwinding, in contrast to proline-kink) also modifies the relative orientation of the side chains at the extracellular side, including residues involved in neurotransmitter binding such as 5.42, 5.43, and 5.46 (Ballesteros et al., 2001b; Deupi et al., 2007). Other membrane proteins also feature this type of helical wide turns (Riek et al., 2008).

Role of TM3 in Stabilizing the Proline-Unwinding of TM5. The analysis of the currently available GPCR crystal structures in the present study allows us to propose a common mechanism by which this unusual conformation of TM5 is stabilized. In bovine rhodopsin, the backbone carbonyl oxygen at position 5.46 is stabilized by a hydrogen bond interaction with $Glu^{3.37}$ (at the interatomic distance of 2.8 Å) and a van der Waals interaction with $Leu^{3.40}$ (3.2 Å) (Fig. 1, A and C) (Li et al., 2004; Deupi et al., 2007). Adenosine A_{2A} receptor preserves similar interactions through $Gln^{3.37}$ (3.2 Å) and $Ile^{3.40}$ (3.9 Å) (Fig. 1G) (Jaakola et al., 2008). It is noteworthy that squid rhodopsin replaces $Glu^{3.37}$ of bovine

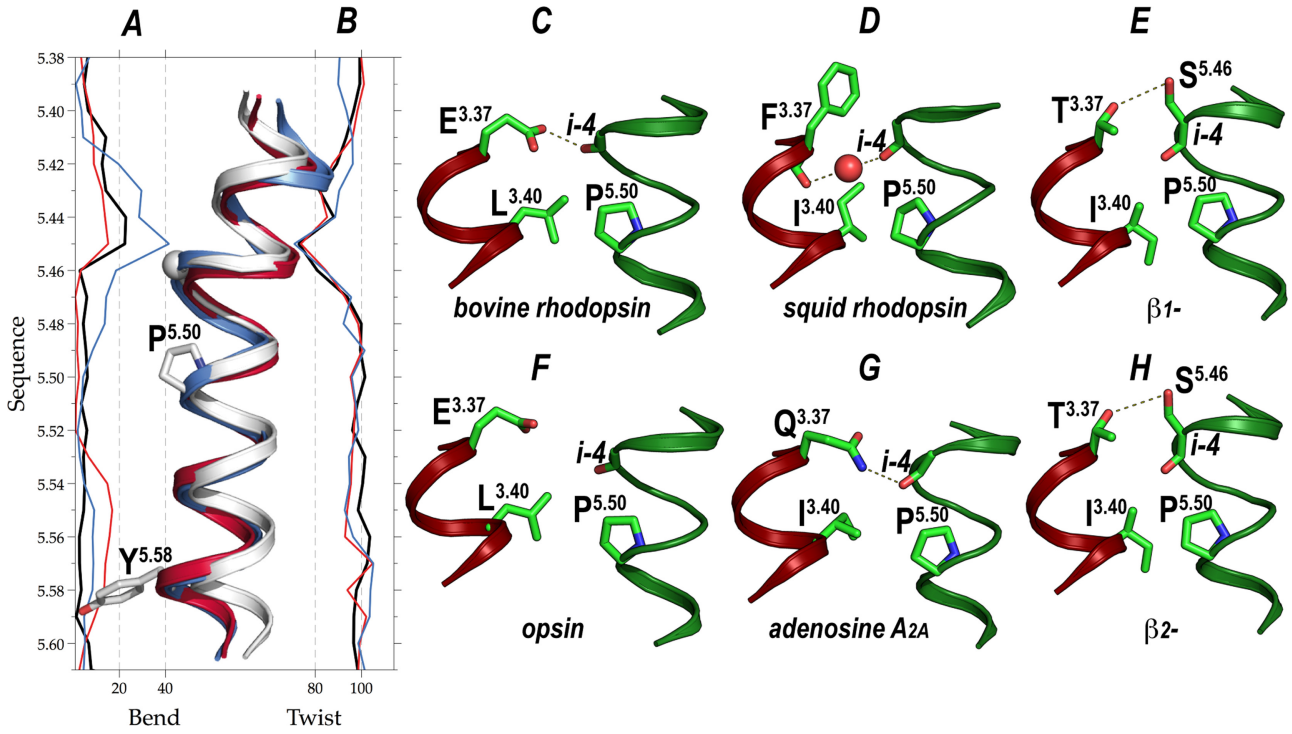

Fig. 1. Comparison of the local opening of transmembrane helix 5 in bovine (Protein Data Bank code1GZM) and squid (Protein Data Bank code 2Z73) rhodopsin, opsin (Protein Data Bank code 3CAP), adenosine A_{2A} (Protein Data Bank code 3EML) and β_1- (Protein Data Bank code 2VT4) and β_2- (2RH1) adrenergic receptors. A and B, evolution of local bend (A) and helical twist (B) angles (in degrees; see *Materials and Methods*) along TM5 in the crystal structures of the β_2-adrenergic receptor (blue), bovine rhodopsin (black), and opsin (red). Residue numbers refer to the first residue in each turn (i.e., the peak of the helical distortion appears in the turn 5.45 to 5.48, labeled as 5.45 in the graphic). C to H, detailed view of the interface between TMs 3 (dark red) and 5 (green) in bovine (C) and squid (D) rhodopsin, opsin (F), adenosine A_{2A} (G), and β_1- (E) and β_2- (H) adrenergic receptors.

TABLE 1

Pharmacological characteristics of hH_1R WT and hH_1R mutants transiently expressed in COS-7 cells

The potency (pEC_{50}) of histamine was measured by NF-κB reporter gene assay. Affinities of [^{3}H]mepyramine (K_D) and H_1R expression levels (B_{max}) are determined by saturation radioligand binding assays. Binding affinity values of H_1R ligands are determined by [^{3}H]mepyramine displacement. Data were calculated as the mean ± S.E.M. (n) indicates the number of experiments, each performed in triplicate.

Receptor	[^{3}H]Mepyramine		Histamine	
	K_D	B_{max}	pK_i	pEC_{50}
	nM	*pmol/mg protein*		
hH_1R WT	1.5 ± 0.2 (7)	14.8 ± 4.6 (7)	5.3 ± 0.1 (4)	6.5 ± 0.1 (5)
$T^{3.37}A$	5.1, 4.5	10.6, 6.5	4.7 ± 0.1 (4)	4.5 ± 0.2 (3)
$T^{3.37}E$	6.1, 6.2	9.6, 15.9	5.1 ± 0.1 (4)	>3.2 (3)
$I^{3.40}A$	10.1 ± 0.3 (3)	9.4 ± 5.1 (3)	5.3 ± 0.2 (4)	>3.4 (3)
$I^{3.40}G$	7.3, 7.6	7.6, 9.8	5.0 ± 0.2 (3)	>3.8 (2)
$S^{3.36}T + I^{3.40}A$	7.8 ± 0.3 (4)	10.4 ± 5.3 (4)	5.4 ± 0.1 (3)	>3.7 (2)
$S^{3.36}T + I^{3.40}G$	3.4 ± 0.2 (3)	13.4 ± 5.0 (3)	5.0 ± 0.1 (3)	>3.9 (2)
$I^{6.40}K + I^{3.40}A$	2.7, 2.1	10.7, 6.5	4.9, 5.4	4.6, 4.5
$I^{6.40}S + I^{3.40}A$	2.2, 1.6	8.7, 5.1	4.6, 5.0	>3.6 (2)

rhodopsin by phenylalanine but presents a discrete water molecule linking the backbone carbonyls at positions 3.37 (3.0 Å) and 5.46 (3.3 Å) (Murakami and Kouyama, 2008) while maintaining the van der Waals interaction between the hydrophobic $Ile^{3.40}$ and the carbonyl oxygen at position 5.46 (3.2 Å) (Fig. 1D). Notably, the recent X-ray structure of opsin (Park et al., 2008) shows that during the process of rhodopsin activation, the hydrogen bond interaction between $Glu^{3.37}$ and the backbone carbonyl (4.9 Å) is disrupted, as previously suggested by NMR measurements of rhodopsin containing ^{13}C-labeled histidine (Patel et al., 2005), whereas $Leu^{3.40}$ has moved slightly away (3.5 Å) (Figs. 1F and 2B). This effect correlates with the minor, but significant, clockwise rotation (viewed from the intracellular side) of TM3 during the process of receptor activation (see *Discussion*). The release of the strong packing of $Leu^{3.40}$ with the 5.45 to 5.48 turn does not result in a change in the local opening of TM5 (Fig. 1B) but in a localized decrease in the bend around $Pro^{5.50}$ (Fig. 1A). In the β_1- (Warne et al., 2008) and β_2- (Rosenbaum et al., 2007) adrenergic receptors, $Ile^{3.40}$ also stabilizes the carbonyl oxygen at position 5.46, similarly to adenosine and opsin receptors, whereas, in this case, the shorter $Thr^{3.37}$ (compared with glutamic acid or glutamine) interacts with the side chain rather than with the backbone carbonyl, of $Ser^{5.46}$ (Figs. 1, E and H, and 2C).

To investigate the role of the amino acids at positions 3.37 and 3.40 in GPCR activation, we have created and studied several H_1R mutants. We have previously used the H_1R as a model system for the study of class A GPCR activation (Bakker et al., 2008). The H_1R belongs to the aminergic subfamily of Class A GPCRs and, like the β_1- and β_2-adrenergic receptors, features $Thr^{3.37}$ and $Ile^{3.40}$ in TM3. Moreover, the H_1R contains a polar $Asn^{5.46}$ amino acid at position 5.46, which is involved in histamine binding (Leurs et al., 1994), linking this GPCR subdomain directly to the agonist binding site.

Influence of $Thr^{3.37}$ and $Ile^{3.40}$ in Agonist-Induced Activation of the Human Histamine H_1R. To test the role of the amino acids at positions 3.37 and 3.40, we engineered mutants in which $Thr^{3.37}$ of the histamine H_1R was substituted by either alanine ($T^{3.37}A$) to remove the hydrogen bonding capability at this position, or glutamic acid ($T^{3.37}E$) to mimic the bovine rhodopsin sequence, and $Ile^{3.40}$ was replaced by either alanine ($I^{3.40}A$) or glycine ($I^{3.40}G$), removing the bulky hydrophobic side chain and, thus, the van der Waals interaction with the carbonyl group at position 5.46. Figure 3D shows the environment of $Thr^{3.37}$ in the β_2-based molecular model of the histamine H_1R (see *Materials and Methods*). $Thr^{3.37}$ forms a hydrogen bond with $Asn^{5.46}$, the binding partner for the imidazole ring of histamine (Leurs et al., 1994), as observed for the $Thr^{3.37}$…$Ser^{5.46}$ interaction in the structure of the β_2-adrenergic receptor (Fig. 1H). Wild-type, $T^{3.37}A$, and $T^{3.37}E$ mutant H_1Rs were well expressed in COS-7 cells at approximately 10 pmol/mg protein as determined by radioligand binding analysis (Table 1). The function of the WT H_1R was evaluated in an NF-κB reporter-gene assay as reported previously (Jongejan et al., 2005; Bakker et al., 2008), and the activation of NF-κB was increased up to 10-fold (E_{max} = 1002 ± 34%) when stimulated with histamine (Fig. 3, A and B). The fact that the functional potency of histamine at WT H_1R exceeds its binding affinity is well in accordance with data published previously (Jongejan et al., 2005; Bakker et al., 2008). Removal of the interaction of $Thr^{3.37}$ with $Asn^{5.46}$, by mutating residue $Thr^{3.37}$ to alanine resulted in a 0.6 log unit decrease of the binding affinity of histamine (pK_i of 5.3 for the WT H_1R versus 4.7 for the $T^{3.37}A$ H_1R) (Table 1), as measured by [^{3}H]mepyramine displacement. A lower constitutive signaling of the $T^{3.37}A$ H_1R mutant compared with that of WT H_1R was observed (Fig. 3, A and B). However, the basal signaling could still be increased by histamine, albeit at higher concentrations (pEC_{50} = 4.5 ± 0.2) (Table 1) (Supplemental Fig. 1). Mutation of residue $Thr^{3.37}$ to glutamic acid (i.e., making this region similar to bovine rhodopsin) did not influence the binding affinity of histamine (Table 1), possibly because $Glu^{3.37}$ maintains both the interaction with $Asn^{5.46}$ (Fig. 3E), as in the WT H_1R (Fig. 3D), and with the carbonyl group at position 5.46, as in bovine rhodopsin (Fig. 1C). Notably, the $T^{3.37}E$ mutant H_1R hardly shows any constitutive activity (Fig. 3, A and B). Moreover, the $T^{3.37}E$ mutant H_1R is activated very poorly by histamine (pEC_{50} > 3.2). Thus, we propose that the additional constraint between $Glu^{3.37}$ and the backbone carbonyl at position 5.46, introduced in the $T^{3.37}E$ mutation, impedes the activation of the mutant H_1R by locking a local structure that cannot be overcome by the agonist histamine.

Removal of the bulky hydrophobic $Ile^{3.40}$ side chain by substitution to alanine or glycine also results in significant effects on both the constitutive activity of the receptor and the process of histamine-induced receptor activation (Fig. 3, A and C). It is noteworthy that these effects are not due to a loss of binding affinity for histamine. As shown in Table 1, both $I^{3.40}A$ and $I^{3.40}G$ mutant H_1Rs are well expressed in COS-7 cells and bind histamine with comparable affinity compared with WT H_1R. The fact that removal of the $Ile^{3.40}$ side chain abolished both the constitutive and histamine-induced activity strongly suggests that this hydrophobic side chain plays a key role in the mechanism of activation. Based

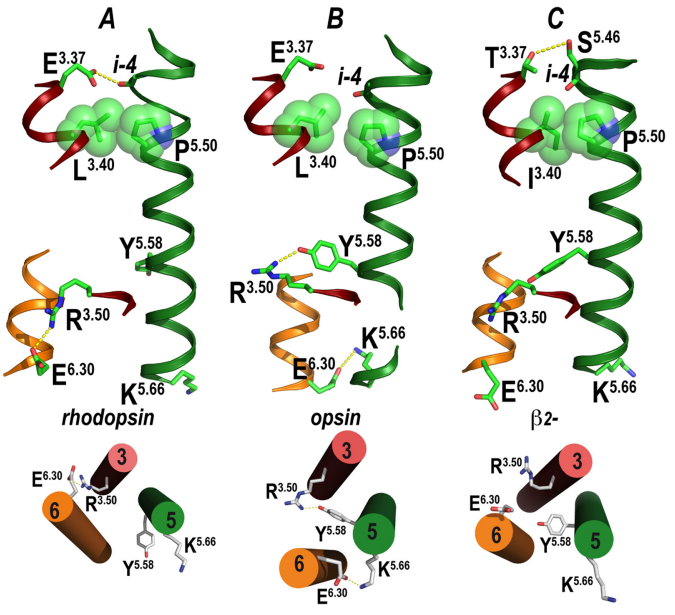

Fig. 2. Packing of transmembrane helix 3 against $Pro^{5.50}$ and network of ionic interactions at the cytoplasmic domain. Packing of the hydrophobic and bulky side chain at position 3.40 with $Pro^{5.50}$ (green spheres) and network of interactions of $Arg^{3.50}$, $Tyr^{5.58}$, $Lys^{5.66}$, and $Glu^{6.30}$ in TMs 3 (dark red), 5 (green), and 6 (yellow) in bovine rhodopsin (A), opsin (B), and the β_2-adrenergic receptor (C) in views parallel (top) and perpendicular (bottom) to the membrane.

on these results and on the recent insights into GPCR structure (Park et al., 2008; Scheerer et al., 2008), we propose that the hydrophobic side chain at position 3.40, which is strongly packed against TM5 (Fig. 2), acts as a pivot and the $Pro^{5.50}$-induced unwinding acts as a hinge in the crucial reorientation of TM5 upon activation, which ultimately facilitates the interactions of $Tyr^{5.58}$ and $Lys^{5.66}$ with $Arg^{3.50}$ and $Glu^{6.30}$, respectively (Fig. 2). Notably, mutations at position 3.40 in rhodopsin are related to retinitis pigmentosa, poor retinal binding, misfolding, reduced expression, decreased time in the MII state, and reduced transducin activation (Madabushi et al., 2004).

To substantiate this hypothesis, we performed two sets of additional experiments. We combined activating point mutations leading to agonist-independent constitutive activity with the inactivating $I^{3.40}A/G$ mutation with the aim to assess their compensatory consequences on receptor function. We have chosen the previously reported $S^{3.36}T$ mutation (Jongejan et al., 2005) in the ligand binding site and the $I^{6.40}K/S$ mutations (Bakker et al., 2008) near the cytoplasmic site, both leading to a large increase in constitutive activity (see *Discussion*). The $S^{3.36}T$ mutation induces the transition of $Trp^{6.48}$ toward TM5 (Jongejan et al., 2005), considered to be the initial stage of the activation process (see below), as observed in the electron microscopy density map of metarhodopsin I (Ruprecht et al., 2004) and in solid-state NMR measurements of metarhodopsin II (Crocker et al., 2006). Thus, we combined the activating $S^{3.36}T$ point mutation with the inactivating $I^{3.40}A/G$ mutation to generate the $S^{3.36}T/I^{3.40}A$ and $S^{3.36}T/I^{3.40}G$ double mutant H_1Rs. The double mutant H_1Rs are well expressed in COS-7 cells and have similar affinity for histamine compared with wild-type H_1R (Table 1). It is noteworthy that both double mutants show lack of constitutive activity and cannot be activated by histamine, resembling the single $I^{3.40}A/G$ mutant H_1R (Fig. 4). On the other hand, the $I^{6.40}S$ and $I^{6.40}K$ mutations induce constitutive receptor activation by triggering the conformational change of $Asn^{7.49}$ toward $Asp^{2.50}$ (Urizar et al., 2005; Bakker

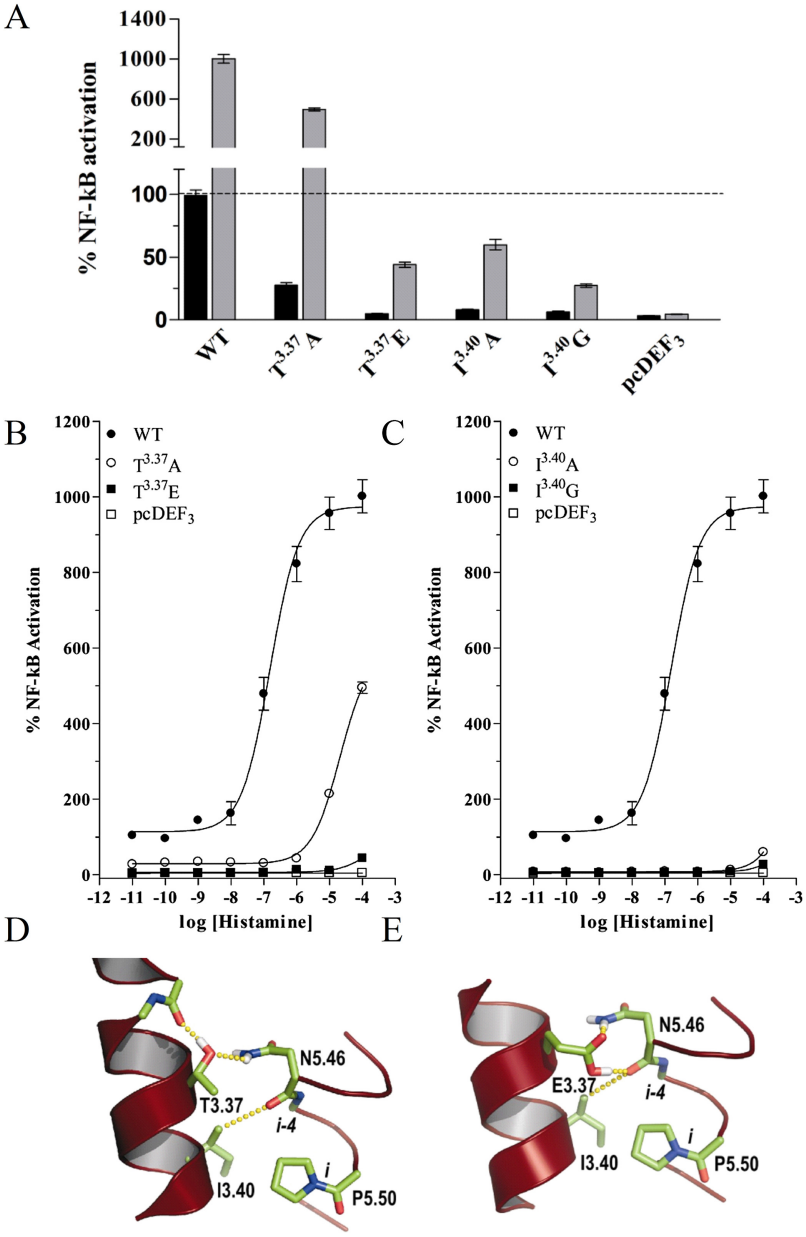

Fig. 3. Influence of $Thr^{3.37}$ and $Ile^{3.40}$ on the agonist-induced activation of the histamine H_1 receptor. NF-κB activation modulated by histamine in COS-7 cells transiently transfected with WT, $Thr^{3.37}$, $Ile^{3.40}$, $Ser^{3.36}$, and empty vector ($pcDEF_3$). All concentration-response curves were constructed with GraphPad Prism version 4.0 ($n \geq 2$, each performed in triplicate). A, basal activity (■) and after stimulation with 10^{-4} M histamine (▨). Results are normalized to the basal activity of WT, which is set to 100%. B, representative concentration-response curves of histamine for WT (●), $T^{3.37}A$ (○), $T^{3.37}E$ (■), and $pcDEF_3$ (□). C, representative concentration-response curves of histamine for WT (●), $I^{3.40}A$ (○), $I^{3.40}G$ (■), and $pcDEF_3$ (□). D and E, detailed view of the interface between TMs 3 and 5 in the molecular model of WT (D) and mutant $T^{3.37}E$ (E) histamine H_1R.

et al., 2008). The $I^{6.40}S$ /$I^{3.40}A$ and $I^{6.40}K$ /$I^{3.40}A$ double mutant H_1Rs show similar affinities for histamine binding (Table 1), but lack constitutive activity and cannot be activated by histamine (Fig. 4). These data reinforce the importance of $Ile^{3.40}$ in the process of receptor activation.

Discussion

A number of studies have provided convincing evidence that GPCRs coexist in different conformations (Kobilka and Deupi, 2007). GPCRs are maintained within an ensemble of inactive conformations through noncovalent interactions between side chains, mostly located in the TM segments (Smit et al., 2007; Rosenbaum et al., 2009) but also at the extracellular surface (Bokoch et al., 2010). Disruption of these stabilizing interactions results in gain-of-function mutations. An evolutionary trace analysis has led to the identification of a putative common signal transduction process for class A GPCRs, in which key residues are grouped into a network of interactions extending from a trigger region near the binding pocket to a coupling region in the cytoplasmic region, connected by an intermediate linking core (Madabushi et al., 2004). This analysis detected $Leu^{3.40}$ of rhodopsin in the trigger region as a structurally and/or functionally important residue.

The fact that the histamine H_1R shows considerable agonist-independent, constitutive signaling, which can be strongly reduced by the inverse agonist mepyramine (Bakker et al., 2001), provides an unique opportunity to approach the mechanism of receptor activation. In this study, we used site-directed mutagenesis of the H_1R to study the proposed role of the hydrophobic side chain at position 3.40, highly conserved in the whole class A of GPCRs, in GPCR activation. Mutation of $Ile^{3.40}$ to either alanine or glycine, removing the bulky side chain, abolished the constitutive activity of the receptor, the effect of constitutive-activity increasing mutations, and the histamine-induced receptor activation, but not the binding of histamine. These data strongly suggest that $Ile^{3.40}$ is not involved in the initial binding step but participates in the subsequent signal propagation upon histamine binding. In the inactive state (Fig. 2, A and C) the hydrophobic side chain at position 3.40 (green surface) is located between the pyrrolidine ring of $Pro^{5.50}$ and the carbonyl oxygen at position 5.46, inducing or stabilizing the local opening of TM5 (Fig. 1B). However, the molecular mechanism by which this residue facilitates receptor activation is not straightforward. The structure of opsin (Park et al., 2008) and previous substituted-cysteine accessibility studies in the β_2-adrenergic receptor (Gether et al., 1997) have shown a clockwise rotation (viewed from the intracellular side) of TM3 during the process of receptor activation. Rotation of TM3 moves the bulky side chain at position 3.40, located between $Pro^{5.50}$ and the 5.46 carbonyl, away from these moieties (Fig. 2B), resulting in a localized decrease of the bend around $Pro^{5.50}$ (Fig. 1A).

Fluorescence spectroscopy experiments used to monitor agonist-induced conformational changes in the β_2-adrenergic receptor provide evidence of a sequential binding model through discrete intermediate conformational states (Swaminath et al., 2004). In an initial step, agonist binding induces relocation of the extracellular side of TM5 to facilitate binding of the hydroxyl groups of the catechol moiety of β_2-adrenergic receptor agonists (Kobilka, 2004). We propose that this movement is transduced as a set of structural rearrangements toward the intracellular side of TM5 with the assistance of $Ile^{3.40}$ acting as a pivot, ultimately enabling the interactions of $Tyr^{5.58}$ with $Arg^{3.50}$ and $Lys^{5.66}$ with $Glu^{6.30}$ in the cytoplasmic side of the receptor (Fig. 5, right arrow). In support of this hypothesis, the $T^{3.37}E$ mutation in the H_1R, which adds an additional constraint between TMs 3 and 5 (Fig. 3E), prevents the transmission of the activation signal through TM5 (Fig. 3B) but does not affect the binding of histamine.

In addition to this activation pathway through TM5, amino acids located in TMs 3 and 6 also participate in other routes of receptor activation (Fig. 5, top left arrow). For instance, agonist binding triggers the $Trp^{6.48}$ rotamer toggle switch from the inactive *g+* (pointing toward TM7) to the active *t* (toward the binding pocket) conformation (Shi et al., 2002; Ruprecht et al., 2004; Crocker et al., 2006; Holst et al., 2010)

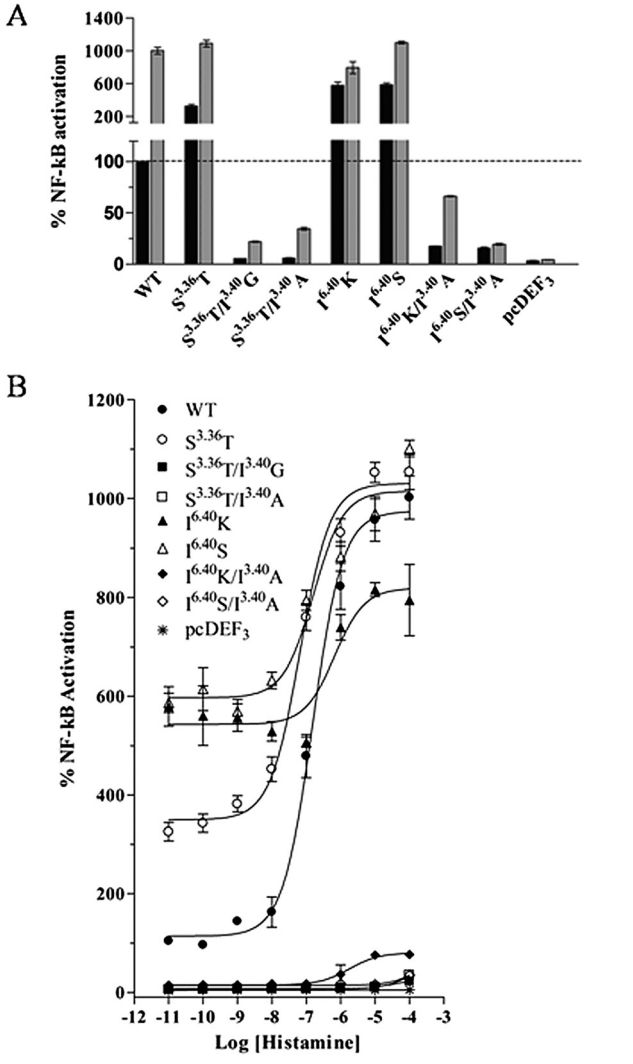

Fig. 4. Influence of double mutants $S^{3.36}T/I^{3.40}G,A$ and $I^{6.40}K,S/I^{3.40}A$ on the agonist-induced activation of the histamine H_1 receptor. NF-κB activation modulated by histamine in COS-7 cells transiently transfected with WT, double H_1R mutants, and empty vector ($pcDEF_3$). All concentration-response curves were constructed with GraphPad Prism version 4.0 ($n \geq 2$, each performed in triplicate). A, basal activity (■) and after stimulation with 10^{-4} M histamine (▨). Results are normalized to the basal activity of WT, which is set to 100%. B, representative concentration-response curves of histamine for WT (●), $S^{3.36}T$ (○), $S^{3.36}T/I^{3.40}G$ (■), $S^{3.36}T/I^{3.40}A$ (□), $I^{6.40}K$ (▲), $I^{6.40}S$ (△), $I^{6.40}K/I^{3.40}A$ (♦), $I^{6.40}S/I^{3.40}A$ (◇), and $pcDEF_3$ (*).

through the formation of specific hydrogen bonds (López-Rodríguez et al., 2005). Notably, the rotamer toggle switch of $Trp^{6.48}$ occurs in a concerted manner with the side chain at position 3.36 from the inactive *t* (toward the binding pocket) to the active *g+* (toward TM7) conformation (Jongejan et al., 2005). To assess whether these pathways of receptor activation are independent or not, we have combined the inactivating $I^{3.40}$A/G mutations (Figs. 4) with the activating $S^{3.36}$T point mutation, which is also located in the trigger region and leads to agonist-independent constitutive activity (Jongejan et al., 2005). The absence of both constitutive activity and histamine-induced activation in these double mutant receptors, despite normal histamine binding, led us to conclude that the movement of TM5 (via the $Ile^{3.40}$ pivot) is essential to stabilize the activation pathway by means of the $Trp^{6.48}$/$Ser^{3.36}$ rotamer toggle switch.

The signal triggered by the $Trp^{6.48}$/$Ser^{3.36}$ toggle switch is transmitted toward intracellular microdomains (Smit et al., 2007; Rosenbaum et al., 2009). In particular, $Asn^{7.49}$ and $Tyr^{7.53}$ (in the NPxxY motif of TM7) undergo conformational changes (Urizar et al., 2005; Park et al., 2008), ultimately leading to the disruption of the ionic interaction between $Arg^{3.50}$ and the adjacent Asp/$Glu^{3.49}$ (the DRY motif of TM3) (Scheer et al., 1996), and an additional Asp/$Glu^{6.30}$ near the cytoplasmic end of TM6 (Ballesteros et al., 2001a) (Fig. 5, bottom left arrow). Disruption of these ionic interactions permits $Arg^{3.50}$ to adopt an extended conformation (Bakker et al., 2008; Park et al., 2008), pointing toward the protein core and to interact with the highly conserved $Tyr^{5.58}$ and $Tyr^{7.53}$ in TMs 5 and 7 (Park et al., 2008). These conformational changes open a cavity between TMs 3, 5, and 6 where the G protein can bind (Scheerer et al., 2008). We have shown previously that mutation of the highly conserved hydrophobic side chain at position 6.40 to glutamic acid, glycine, alanine, arginine, lysine, or serine results in highly constitutively active receptors for which almost no additional histamine-induced receptor activation can be detected (Bakker et al., 2008). These substitutions at position 6.40 seem to modify the conformation of the key $Asn^{7.49}$, $Tyr^{7.53}$, and $Arg^{3.50}$ side chains, located in the coupling region near the G protein binding site (Bakker et al., 2008). Notably, adding the $I^{3.40}$A mutation, in the trigger region, to the constitutively active $I^{6.40}$S/K mutant receptors decreases constitutive activity and impedes histamine-induced receptor activation (Fig. 4). These results suggest a key role of $Ile^{3.40}$ in transmitting the activating signal from the binding pocket to the cytoplasmic side and in stabilizing the conformational changes of TM5 at the intracellular side of the receptor, probably by means of $Tyr^{5.58}$.

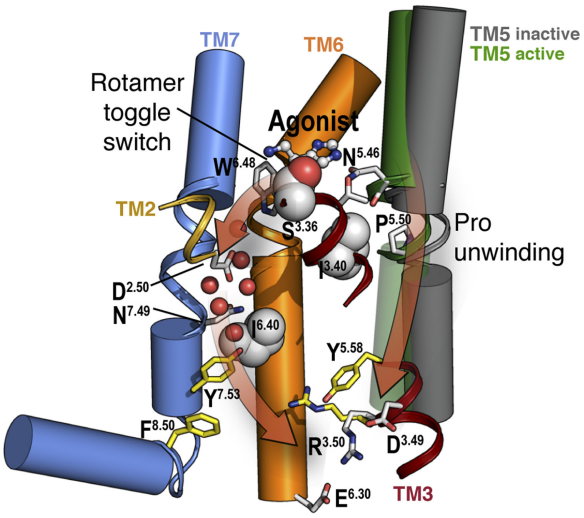

Fig. 5. Pathways of activation in class A GPCRs. Agonist (shown as ball-and-sticks) binding leads to conformational changes at the extracellular domain that are transmitted (arrows) toward the cytoplasmic domain of the receptor. The right arrow represents how the interaction of agonists with the extracellular side of TM5 is transduced toward the intracellular side with the assistance of $Ile^{3.40}$ (shown as spheres) and the $Pro^{5.50}$-induced unwinding of TM5, facilitating the interaction of $Tyr^{5.58}$ with $Arg^{3.50}$ in the active state (yellow sticks). Agonist binding may also trigger the $Trp^{6.48}$/$Ser^{3.36}$ rotamer toggle switch (top/left arrow). This agonist-induced signal is transmitted through a conserved water cluster (red spheres) toward intracellular microdomains like $Asn^{7.49}$ and $Tyr^{7.53}$ of the NPxxY motif (bottom/left arrow), facilitating the interaction of $Tyr^{7.53}$ with $Arg^{3.50}$ in the active state (yellow sticks). Disruption of the ionic interactions between $Arg^{3.50}$ and the adjacent $Asp^{3.49}$ (the DRY motif of TM3) and an additional $Glu^{6.30}$ facilitates the movement of TM6 (not shown), opening a cavity in which the G protein can bind (data not shown). Side chains of amino acids modeled in inactive conformations are depicted in white, in their putative active conformations in yellow, and the side chains of $Ser^{3.36}$, $Ile^{3.40}$, and $Ile^{6.40}$, which are discussed in this article, are depicted as spheres.

Triggering specific pathways along the activation process might be an explanation for the observed collateral efficacy of GPCR agonists. Our data provide further insight in the molecular mechanisms of GPCR activation, and we propose that one of such additional pathways consists in the agonist-induced relocation of the extracellular side of TM5 toward the transmembrane bundle. The activation-signal is then further propagated toward the cytoplasmic region through the fulcrum/lever mechanism described above, in which $Pro^{5.50}$ acts as a hinge and the highly conserved hydrophobic $Ile^{3.40}$ side chain acts as a pivot.

Authorship Contributions

Participated in research design: Sansuk, Bakker, Jongejan, Pardo, and Leurs.

Conducted experiments: Sansuk, Torrecillas, and Nijmeijer.

Performed data analysis: Sansuk, Deupi, Torrecillas, and Nijmeijer.

Wrote or contributed to the writing of the manuscript: Sansuk, Deupi, Bakker, Pardo, and Leurs.

References

Bakker RA, Jongejan A, Sansuk K, Hacksell U, Timmerman H, Brann MR, Weiner DM, Pardo L, and Leurs R (2008) Constitutively active mutants of the histamine H_1 receptor suggest a conserved hydrophobic asparagine-cage that constrains the activation of class A G protein-coupled receptors. *Mol Pharmacol* **73:**94–103.

Bakker RA, Schoonus SB, Smit MJ, Timmerman H, and Leurs R (2001) Histamine H_1-receptor activation of nuclear factor-kappa B: roles for $G\beta\gamma$- and $G\alpha_{(q/11)}$-subunits in constitutive and agonist-mediated signaling. *Mol Pharmacol* **60:**1133–1142.

Ballesteros JA, Jensen AD, Liapakis G, Rasmussen SG, Shi L, Gether U, and Javitch JA (2001a) Activation of the β_2-adrenergic receptor involves disruption of an ionic lock between the cytoplasmic ends of transmembrane segments 3 and 6. *J Biol Chem* **276:**29171–29177.

Ballesteros JA, Shi L, and Javitch JA (2001b) Structural mimicry in G protein-coupled receptors: implications of the high-resolution structure of rhodopsin for structure-function analysis of rhodopsin-like receptors. *Mol Pharmacol* **60:**1–19.

Ballesteros JA and Weinstein H (1995) Integrated methods for the construction of three dimensional models and computational probing of structure-function relations in G-protein coupled receptors. *Methods Neurosci* **25:**366–428.

Bansal M, Kumar S, and Velavan R (2000) HELANAL: a program to characterize helix geometry in proteins. *J Biomol Struct Dyn* **17:**811–819.

Bokoch MP, Zou Y, Rasmussen SG, Liu CW, Nygaard R, Rosenbaum DM, Fung JJ, Choi HJ, Thian FS, Kobilka TS, et al. (2010) Ligand-specific regulation of the extracellular surface of a G-protein-coupled receptor. *Nature* **463:**108–112.

Bradford MM (1976) A rapid and sensitive method for the quantitation of microgram quantities of protein utilizing the principle of protein-dye binding. *Anal Biochem* **72:**248–254.

Crocker E, Eilers M, Ahuja S, Hornak V, Hirshfeld A, Sheves M, and Smith SO

(2006) Location of Trp265 in metarhodopsin II: implications for the activation mechanism of the visual receptor rhodopsin. *J Mol Biol* **357:**163–172.
Deupi X, Dölker N, López-Rodríguez ML, Campillo M, Ballesteros JA, and Pardo L (2007) Structural models of class a G protein-coupled receptors as a tool for drug design: insights on transmembrane bundle plasticity. *Curr Top Med Chem* **7:**991–998.
Deupi X, Olivella M, Govaerts C, Ballesteros JA, Campillo M, and Pardo L (2004) Ser and Thr residues modulate the conformation of pro-kinked transmembrane alpha-helices. *Biophys J* **86:**105–115.
Fukui H, Fujimoto K, Mizuguchi H, Sakamoto K, Horio Y, Takai S, Yamada K, and Ito S (1994) Molecular cloning of the human histamine H_1 receptor gene. *Biochem Biophys Res Commun* **201:**894–901.
Gether U, Lin S, Ghanouni P, Ballesteros JA, Weinstein H, and Kobilka BK (1997) Agonists induce conformational changes in transmembrane domains III and VI of the β_2 adrenoceptor. *EMBO J* **16:**6737–6747.
Goldman LA, Cutrone EC, Kotenko SV, Krause CD, and Langer JA (1996) Modifications of vectors pEF-BOS, pcDNA1 and pcDNA3 result in improved convenience and expression. *Biotechniques* **21:**1013–1015.
Holst B, Nygaard R, Valentin-Hansen L, Bach A, Engelstoft MS, Petersen PS, Frimurer TM, and Schwartz TW (2010) A conserved aromatic lock for the tryptophan rotameric switch in TM-VI of seven-transmembrane receptors. *J Biol Chem* **285:**3973–3985.
Jaakola VP, Griffith MT, Hanson MA, Cherezov V, Chien EY, Lane JR, Ijzerman AP, and Stevens RC (2008) The 2.6 angstrom crystal structure of a human A_{2A} adenosine receptor bound to an antagonist. *Science* **322:**1211–1217.
Jongejan A, Bruysters M, Ballesteros JA, Haaksma E, Bakker RA, Pardo L, and Leurs R (2005) Linking ligand binding to histamine H_1 receptor activation. *Nat Chem Biol* **1:**98–103.
Kobilka B (2004) Agonist binding: a multistep process. *Mol Pharmacol* **65:**1060–1062.
Kobilka BK and Deupi X (2007) Conformational complexity of G-protein-coupled receptors. *Trends Pharmacol Sci* **28:**397–406.
Kristiansen K (2004) Molecular mechanisms of ligand binding, signaling, and regulation within the superfamily of G-protein-coupled receptors: molecular modeling and mutagenesis approaches to receptor structure and function. *Pharmacol Ther* **103:**21–80.
Leurs R, Smit MJ, Tensen CP, Ter Laak AM, and Timmerman H (1994) Site-directed mutagenesis of the histamine H_1-receptor reveals a selective interaction of asparagine207 with subclasses of H_1-receptor agonists. *Biochem Biophys Res Commun* **201:**295–301.
Li J, Edwards PC, Burghammer M, Villa C, and Schertler GF (2004) Structure of bovine rhodopsin in a trigonal crystal form. *J Mol Biol* **343:**1409–1438.
López-Rodríguez ML, Morcillo MJ, Fernández E, Benhamú B, Tejada I, Ayala D, Viso A, Campillo M, Pardo L, Delgado M, et al. (2005) Synthesis and structure-activity relationships of a new model of arylpiperazines. 8. Computational simulation of ligand-receptor interaction of 5-HT(1A)R agonists with selectivity over α_1-adrenoceptors. *J Med Chem* **48:**2548–2558.
Madabushi S, Gross AK, Philippi A, Meng EC, Wensel TG, and Lichtarge O (2004) Evolutionary trace of G protein-coupled receptors reveals clusters of residues that determine global and class-specific functions. *J Biol Chem* **279:**8126–8132.
Martí-Renom MA, Stuart AC, Fiser A, Sánchez R, Melo F, and Sali A (2000) Comparative protein structure modeling of genes and genomes. *Annu Rev Biophys Biomol Struct* **29:**291–325.
Murakami M and Kouyama T (2008) Crystal structure of squid rhodopsin. *Nature* **453:**363–367.
Pardo L, Deupi X, Dölker N, López-Rodríguez ML, and Campillo M (2007) The role of internal water molecules in the structure and function of the rhodopsin family of G protein-coupled receptors. *Chembiochem* **8:**19–24.
Park JH, Scheerer P, Hofmann KP, Choe HW, and Ernst OP (2008) Crystal structure of the ligand-free G-protein-coupled receptor opsin. *Nature* **454:**183–187.
Patel AB, Crocker E, Reeves PJ, Getmanova EV, Eilers M, Khorana HG, and Smith SO (2005) Changes in interhelical hydrogen bonding upon rhodopsin activation. *J Mol Biol* **347:**803–812.
Riek RP, Finch AA, Begg GE, and Graham RM (2008) Wide turn diversity in protein transmembrane helices implications for G-protein-coupled receptor and other polytopic membrane protein structure and function. *Mol Pharmacol* **73:**1092–1104.
Rosenbaum DM, Cherezov V, Hanson MA, Rasmussen SG, Thian FS, Kobilka TS, Choi HJ, Yao XJ, Weis WI, Stevens RC, et al. (2007) GPCR engineering yields high-resolution structural insights into β_2-adrenergic receptor function. *Science* **318:**1266–1273.
Rosenbaum DM, Rasmussen SG, and Kobilka BK (2009) The structure and function of G-protein-coupled receptors. *Nature* **459:**356–363.
Ruprecht JJ, Mielke T, Vogel R, Villa C, and Schertler GF (2004) Electron crystallography reveals the structure of metarhodopsin I. *EMBO J* **23:**3609–3620.
Scheer A, Fanelli F, Costa T, De Benedetti PG, and Cotecchia S (1996) Constitutively active mutants of the α_{1B}-adrenergic receptor: role of highly conserved polar amino acids in receptor activation. *EMBO J* **15:**3566–3578.
Scheerer P, Park JH, Hildebrand PW, Kim YJ, Krauss N, Choe HW, Hofmann KP, and Ernst OP (2008) Crystal structure of opsin in its G-protein-interacting conformation. *Nature* **455:**497–502.
Shi L, Liapakis G, Xu R, Guarnieri F, Ballesteros JA, and Javitch JA (2002) β_2 adrenergic receptor activation. Modulation of the proline kink in transmembrane 6 by a rotamer toggle switch. *J Biol Chem* **277:**40989–40996.
Smit MJ, Vischer HF, Bakker RA, Jongejan A, Timmerman H, Pardo L, and Leurs R (2007) Pharmacogenomic and structural analysis of constitutive G protein-coupled receptor activity. *Annu Rev Pharmacol Toxicol* **47:**53–87.
Swaminath G, Xiang Y, Lee TW, Steenhuis J, Parnot C, and Kobilka BK (2004) Sequential binding of agonists to the β_2 adrenoceptor. Kinetic evidence for intermediate conformational states. *J Biol Chem* **279:**686–691.
Urizar E, Claeysen S, Deupí X, Govaerts C, Costagliola S, Vassart G, and Pardo L (2005) An activation switch in the rhodopsin family of G protein-coupled receptors: the thyrotropin receptor. *J Biol Chem* **280:**17135–17141.
Warne T, Serrano-Vega MJ, Baker JG, Moukhametzianov R, Edwards PC, Henderson R, Leslie AG, Tate CG, and Schertler GF (2008) Structure of a β_1-adrenergic G-protein-coupled receptor. *Nature* **454:**486–491.

Address correspondence to: Dr. Rob Leurs, Leiden/Amsterdam Center for Drug Research, Department of Medicinal Chemistry, Vrije Universiteit Amsterdam, De Boelelaan 1083, 1081HV Amsterdam, the Netherlands. E-mail: leurs@few.vu.nl